case of a rigid rotor supported on full circular bearings. The bearings are represented by both short and long-bearing approximations, and the resulting nonlinear equations of motion are solved both numerically and by analog computer. The applicability of the rather extensive simulation results presented is limited, however, by the basic assumption that the extent of the lubricant film is 360 deg. The present work determines for similar bearing length assumptions the locations of the boundaries of the positive film pressure region (180 deg) based upon journal center location and velocity. Results obtained are thus more nearly representative of the characteristics of common bearing types in which film rupture occurs.

Lund's [2] linearized, short-bearing study is one of the first works to include the effects of rotor dimensions and mass distribution upon rotor-bearing system stability. His comprehensive analytical treatment, in which the conical mode of instability is also taken into account, presents methods by which small amplitude whirl orbit sizes may be evaluated. Lund does not employ simulation as a means of solution, but instead uses the Method of Averaging to obtain stability information. The present work yields results comparable at least to those of the plane-motion portions of Lund's work, and has the added advantage of being able to calculate transient motions.

References

1 Hori, Y., "A Theory of Oil Whip," *Journal of Applied Mechanics*, Vol. 26, TRANS. ASME, Vol. 81, Series E, June 1959, p. 189.

2 Lund, J. W., "Self-Excited Stationary Whirl Orbits of a Journal in a Sleeve Bearing," PhD Thesis, Rensselaer Polytechnic Institute, Troy, N. Y., 1966.

3 Booker, J. F., "Dynamically Loaded Journal Bearings: Mobility Method of Solution," *Journal of Basic Engineering*, TRANS. ASME, Vol. 87, No. 3, 1965, p. 537.

4 Booker, J. F., "A Table of the Journal Bearing Integral," *Journal of Basic Engineering*, TRANS ASME, Vol. 87, No. 2, 1965, p. 533.

5 Badgley, R. H., "Turborotor Instability—Dynamic Unbalance, Gyroscopic, and Variable Speed Effects with Finite-Length, Cavitated, Fluid-Film Bearings," PhD Thesis, Cornell University, Ithaca, N. Y., 1967.

6 Reddi, M. M., and Trumpler, P. R., "Stability of the High-Speed Journal Bearing Under Steady Load—1. The Incompressible Film," *Journal of Engineering for Industry*, TRANS. ASME, Vol. 84, 1962.

7 Holmes, R., "The Vibration of a Rigid Shaft on Short Sleeve Bearings," *Journal of Mechanical Engineering Science*, Vol. 2, No. 4, 1960, p. 337.

8 Huggins, N. J., "Nonlinear Modes of Vibration of a Rigid Rotor in Short Journal Bearings," Paper 18, *Proceedings of the Second Lubrication and Wear Convention*, Institution of Mechanical Engineers, London, 1964.

9 Mitchell, J. R., Holmes, R., and Byrne, J., "Oil Whirl of a Rigid Rotor in 360 deg Journal Bearings: Further Characteristics," *Proceedings of the Institution of Mechanical Engineers*, Vol. 180, Pt. 1, No. 25, 1965–66.

10 McCormick, J. M., and Salvadori, M. G., *Numerical Methods in FORTRAN*, Prentice-Hall, Englewood Cliffs, N. J., Feb. 1965.

11 Jennings, U. D., and Ocvirk, F. W., "The Simulation of Bearing Whirl on an Electronic Analog Computer," *Journal of Basic Engineering*, TRANS. ASME, Series D, Vol. 84, 1962, p. 503.

DISCUSSION

V. Castelli[4]

The authors have presented an interesting analytical technique for the investigation of plain journal bearing instability limits. They have given closed-form solutions for the film forces for each of the major bearing models, and have proceeded to utilize them in a nonlinear extrapolation solution of the equations of motion. The results obtained, especially those for the short bearing under conditions of small initial displacement, might have been compared more closely with the recent work of J. W. Lund, the authors' reference [2]. (Important parts of that work appear in J. W. Lund and E. Saibel, "Oil Whip Whirl Orbits of a Rotor in Sleeve Bearings," ASME Paper No. 67-Vibr-28.)

Results of both of these studies should compare rather closely, since almost identical bearing models were used by them. Their major differences involved the methods of solution, in that Lund utilized a linearized perturbation technique.

[4] Professor of Mechanical Engineering, Columbia University, New York, N. Y.

E. J. Gunter, Jr.,[5] and R. G. Kirk[6]

The authors are to be congratulated for their excellent work on the stability of the bearing system presented in this paper. The equations of motion have been formulated in the standard rotating coordinate system to consider only a balanced horizontal rotor. At the University of Virginia we have formulated an analysis based on the short bearing assumption to include rotor unbalance, unidirectional, and rotating loads. Analysis indicates that the addition of a unidirectional external load can considerably extend the rotor stability speed. Therefore a more appropriate stability parameter for Fig. 3 should be $\omega\sqrt{MC/W}$, where W is

[5] Associate Professor of Mechanical Engineering, University of Virginia, Charlottesville, Va. Mem. ASME.

[6] National Defense Fellow, University of Virginia.

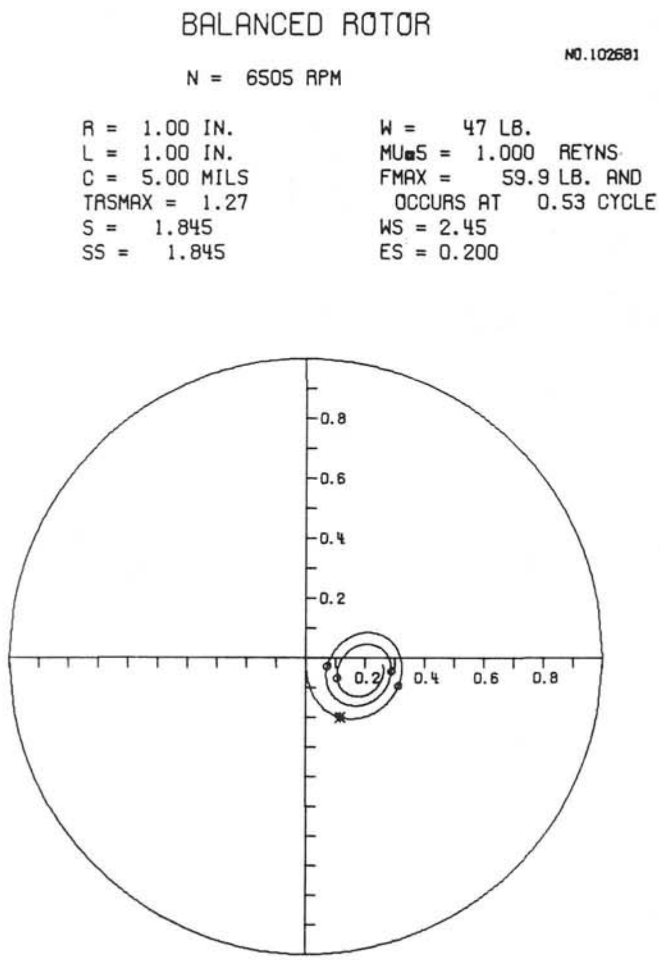

Fig. 10

Copyright © 1969 by ASME

Downloaded from http://verification.asmedigitalcollection.asme.org/tribology/article-pdf/91/4/630/5629874/630_1.pdf by guest on 01 December 2023

Check for updates

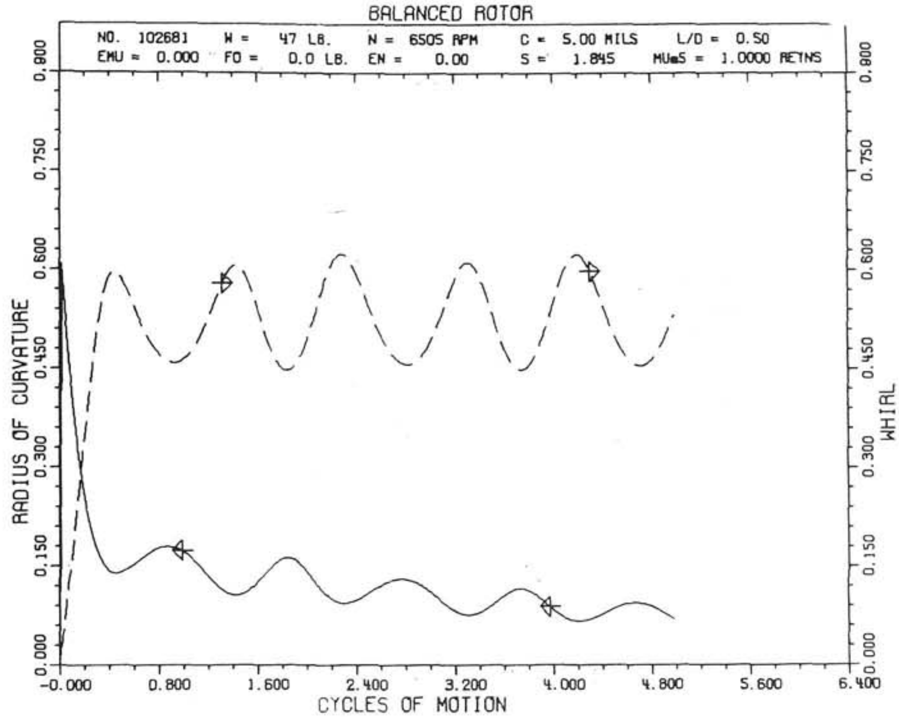

Fig. 11

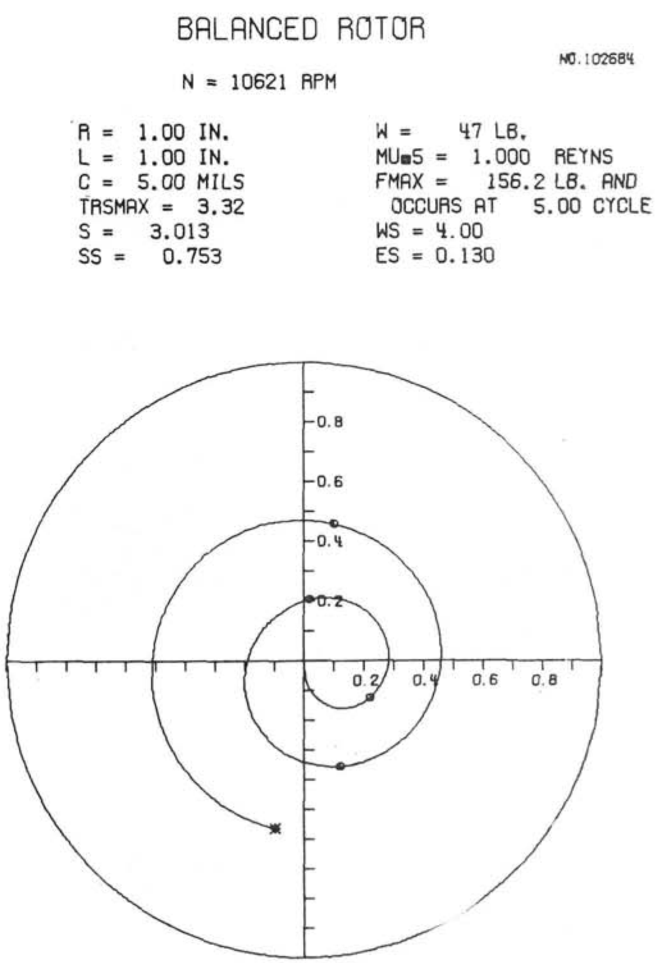

Fig. 12

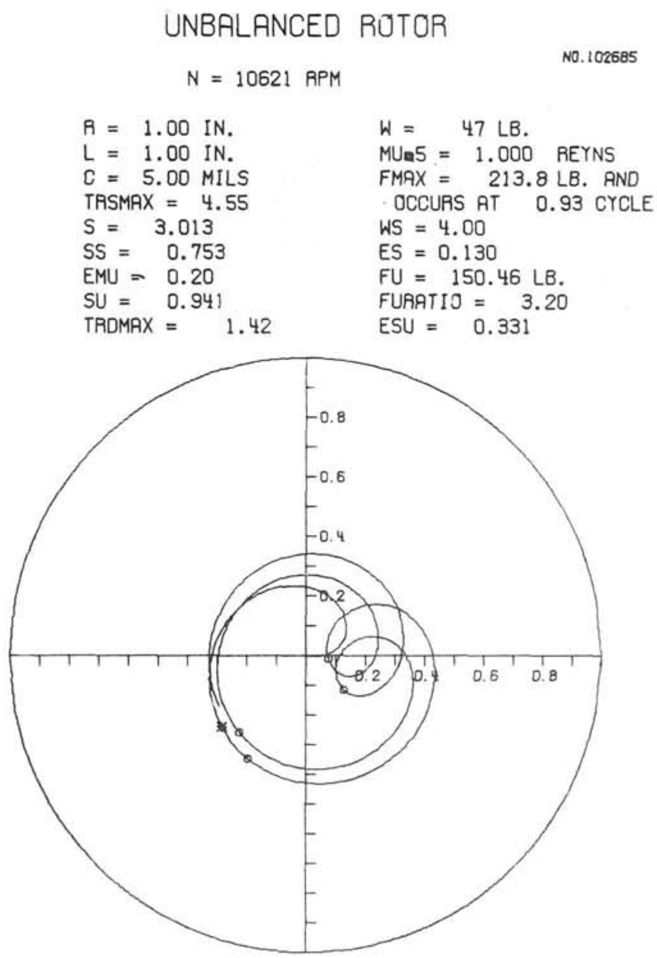

Fig. 13

Downloaded from http://verification.asmedigitalcollection.asme.org/tribology/article-pdf/91/4/630/5629874/630_1.pdf by guest on 01 December 2023

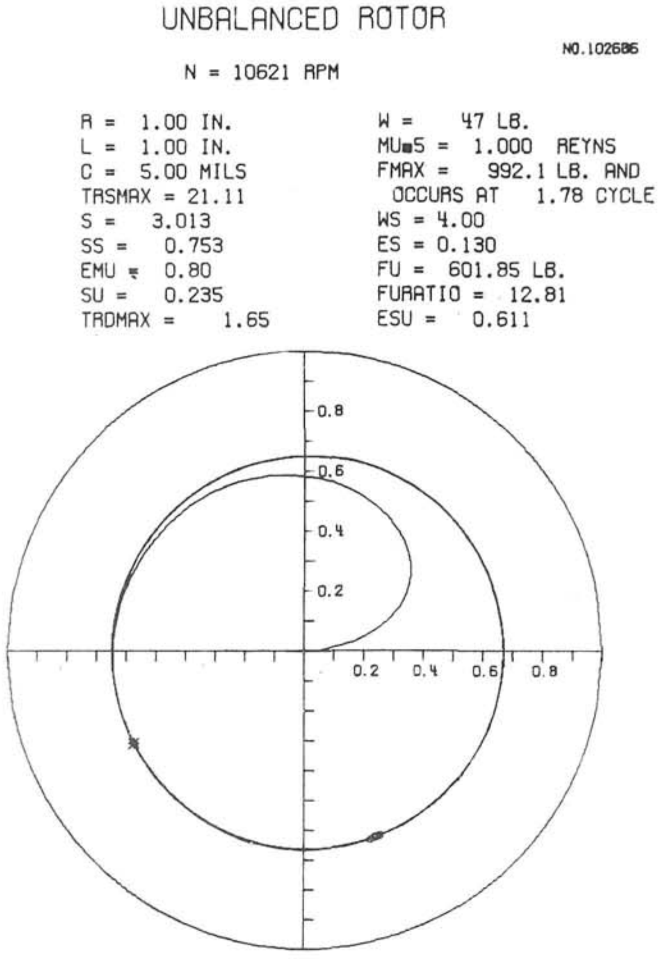

Fig. 14

the resultant unidirectional load. This dimensionless parameter is similar to the stability parameter of $N\sqrt{\frac{MC}{W}}$ as used by Reddi and Trumpler [6].

The computer program developed by the writers integrates the resulting nonlinear equations by a fourth-order Runge-Kutta procedure. The calculated journal center orbit is plotted relative to the bearing clearance by a Calcomp plotter procedure. For example, Fig. 10 represents journal motion similar to Fig. 2 in which the equilibrium eccentricity $\epsilon_o = 0.2$ and the stability threshold $\omega_j/\omega_g = W_s = 2.45$. Note that the orbit is stable and will eventually reach a steady state eccentricity of 0.2.

In Fig. 2, the authors show a plot of R versus time. It appears that R is the radius vector drawn from the steady-state equilibrium position to the instantaneous journal center. In the case where rotor unbalance or time varying external loads are also considered, a steady-state equilibrium position is nonexistent. In our computer program we have calculated the instantaneous radius of curvature and precession rate of the orbit. Fig. 11 represents a plot of the dimensionless radius of curvature ρ/C and whirl ratio $\dot{\phi}/\omega$ for the journal orbit as shown in Fig. 10. After 5 shaft revolutions the orbit radius of curvature R is between 0.06 to 0.09 which is similar to the values shown by the authors in Fig. 2 after 31 radians. Notice that in Fig. 11, the precession or whirl ratio for a horizontal rotor is not constant but varies cyclically between 0.45 and 0.63. We have been able to obtain a constant whirl speed only for the case of a vertical rotor.

Another important characteristic of the bearing system is the hydrodynamic forces generated. The resultant hydrodynamic bearing force for each time step is calculated and the maximum value for the run interval is recorded. An asterisk is placed on the orbit to denote the occurrence of the maximum bearing force. For example, the maximum force is 59.9 lb and occurs at 0.53 cycles of shaft motion. A dot is placed on the trajectory after each shaft revolution. This dot simulates a key phasor or timing mark as used in experimental bearing test rigs to indicate synchronous or nonsynchronous precession.

Fig. 12 represents the rotor motion with the speed increased to 10,621 rpm. In this case the stability parameter is 4.00 and the rotor is unstable as predicted by Fig. 3. The maximum force developed is 156 lb and occurs at the end of 5 cycles. The motion will eventually form a limit cycle after approximately 10 cycles. If an external load of 150 lb is applied to the rotor ($W_s = 2.00$), the rotor will stabilize at an eccentricity of 0.40.

Fig. 13 represents the journal motion with the addition of light unbalance. Note the formation of a limit cycle and the characteristic fractional frequency whirl orbit.

If the rotor unbalance is sufficiently increased, the rotor orbit may be stabilized to synchronous precession only, as shown in Fig. 14. Notice that all the timing dots occur at the same location indicating synchronous motion. In this case we see that the maximum force developed is 992 lb which is 21 times greater than the rotor weight (TRSMAX = 21). Thus it appears undesirable to stabilize the rotor orbit by the addition of shaft unbalance because of the large forces transmitted.

Authors' Closure

Dr. Castelli's comments with regard to the work of Lund, reference [2], are quite appropriate. A comparison of the short bearing initial-displacement instability threshold curve of Fig. 3 with the threshold curves obtained by Lund is one means by which the two methods of solution may be directly contrasted. The comparison is made via Lund's Fig. 6, which is reproduced herein as Fig. 15. The abscissas of Fig. 3 and Fig. 15 are the same. Further, under gravity loading, $Mg = W$ and the ordinates are related by the following expression:

$$\frac{CM\omega^2}{W} = \frac{C\omega^2}{g} = \frac{\omega^2}{\omega_g^{\,2}} \equiv \left(\frac{\omega_j}{\omega_g}\right)^2$$

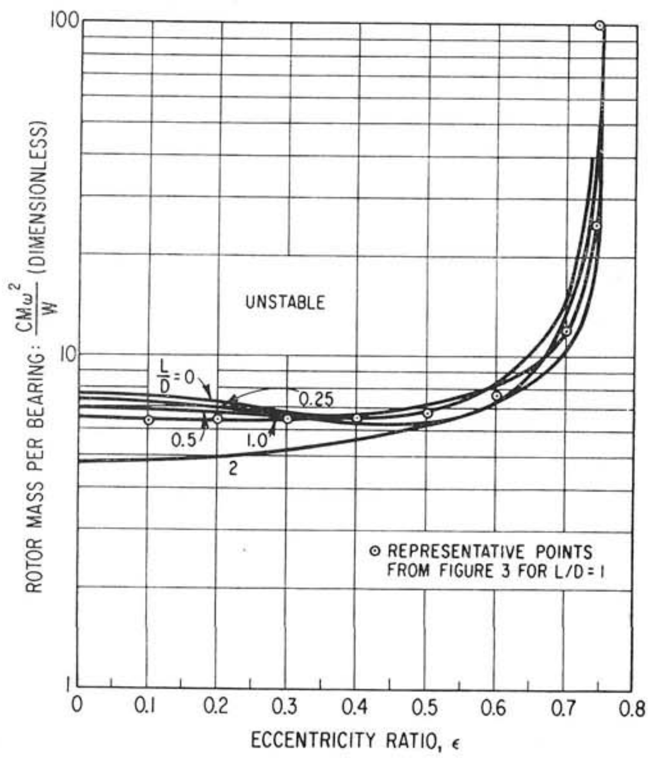

Fig. 15 The threshold of instability of the equilibrium position as a function of the L/D-ratio (from reference [2], Fig. 6)

Downloaded from http://verification.asmedigitalcollection.asme.org/tribology/article-pdf/91/4/630/5629874/630_1.pdf by guest on 01 December 2023

Thus values of ω_j/ω_g from Fig. 3, which were obtained for $L/D = 1$, may be squared and plotted directly in Fig. 15. Representative values obtained in this manner are shown as circled points. The agreement is excellent for eccentricity ratios below about 0.4. Between 0.4 and 0.7, the results shown in Fig. 3 are slightly conservative compared to those of Lund (in that they predict a somewhat lower threshold speed). For eccentricity ratios greater than 0.7 and at values of Rotor Mass per Bearing lower than about 25.0, agreement is again excellent. At values much greater than 25.0, the threshold curve of Fig. 3 becomes asymptotic to eccentricity ratio equal to 0.74, while Lund's $L/D = 1$ curve appears to be asymptotic to 0.76.

The detailed discussion presented by Dr. Gunter and Mr. Kirk is particularly interesting. The results presented in Figs. 10 and 12 for two typical designs appear to complement the results of Figs. 2 and 3 in a useful way. The studies of instantaneous radius of curvature and precession rate of the orbits shed some light upon the fundamental dynamic behavior of the journal at or near the threshold of instability. Perhaps more important, however, is the discussion of the stabilizing effect of dynamic unbalance. A parameter study of this quantity should prove to be particularly valuable as a design tool. It should be noted in passing that the ϵ, ϕ polar coordinate system used for the original study is fixed, *not* rotating (as implied by the discussion). While the polar coordinate system is incompatible with the rectangular coordinate system usually used to describe support behavior, and will experience numerical difficulties at the origin, a coordinate transformation is sufficient to correct either difficulty. Finally, the stability parameter ω_j/ω_g is completely equivalent to the parameter $\omega\sqrt{MC/W}$, and the effects of additional external dead load may be studied by varying the gravitational constant $g \equiv W/M$.

Downloaded from http://verification.asmedigitalcollection.asme.org/tribology/article-pdf/91/4/630/5629874/630_1.pdf by guest on 01 December 2023